Thermal Conductivity of Gaseous Difluoromethane and Pentafluoroethane near the Saturation Line

Li-Qun Sun, Ming-Shan Zhu,* Li-Zhong Han, and Zhao-Zhuang Lin

Department of Thermal Engineering, Tsinghua University, Beijing, 100084, P. R. China

The paper reports the measurements of the thermal conductivity of gaseous difluoromethane (HFC-32) over the temperature range 254.51 K to 341.76 K and the thermal conductivity of gaseous pentafluoroethane (HFC-125) over the temperature range 251.21 K to 333.70 K near the saturation line. The thermal conductivities were measured in a transient hot-wire instrument employing two anodized tantalum wires as the heat source with an uncertainty of 3%. The results were correlated as a function of temperature and compared with the results from the literature.

Introduction

Mixtures containing difluoromethane (HFC-32) or pentafluoroethane (HFC-125) are considered as potential alternatives to replace chlorodifluoromethane (HCFC-22). However, measurements on the thermal conductivities of gaseous HFC-32 and HFC-125 are very limited. Tanaka et al. measured the thermal conductivity of gaseous HFC-32, HFC-125, and their mixtures (Tanaka, 1995). Tsvetkov et al. measured the thermal conductivity of gaseous HFC-125 at low density (Tsvetkov, 1995). Gross et al. measured the thermal conductivity of gaseous HFC-32 and HFC-125 to 345 K and 335 K, respectively (Gross and Song, 1996). In this paper, a transient hot-wire instrument employing two anodized tantalum wires as the heat source was set up and absolute measurements of thermal conductivities of gaseous HFC-32 and HFC-125 near the saturation line are reported with an uncertainty of 3%.

Working Equation

The theory of the transient hot-wire technique for gas thermal conductivity measurements has been given in detail elsewhere (Healy, 1976). According to the theory, the thermal conductivity, λ, of the fluid can be obtained with the following equations

$$\Delta T_{\mathrm{id}} = \Delta T_{\mathrm{w}} + \sum \delta T_i = \frac{q}{4\pi\lambda(T_{\mathrm{r}},\rho_{\mathrm{r}})} \ln \frac{4kt}{a^2 C} \qquad (1)$$

and

$$T_{\mathrm{r}} = T_0 + \frac{1}{2}(\Delta T_1 + \Delta T_2) \qquad (2)$$

where T_0 is the equilibrium temperature of the fluid before heating, T_{r} is the reference temperature, ρ_{r} is the density of the fluid at the reference temperature T_{r} and the primary pressure P_0, q is the energy input per unit length of the hot wires, t is the time of heating, a is the wire radius, λ is the thermal conductivity of the fluid under the condition of T_{r} and P_0, ΔT_{id} is the temperature rise of the hot wire under the ideal conditions, ΔT_{w} is the temperature rise of the hot wire under the experimental conditions, ΔT_1 and ΔT_2 refer to the temperature rise of the hot-wire at the initial moment and the final moment, respectively, and C is a numerical constant. The symbol k represents the thermal diffusivity of the fluid surrounding the wires. The various correction terms δT_i have been identified (Healy, 1976) and are all rendered less than 1% of ΔT_{id} except the correction term induced by the thermophysical properties of the hot wire which is rendered less than 3% of ΔT_{id} in the interested time range by the design of the wires and the operation of the instrument. It follows from eq 1 that an essential feature of the correct operation of the instrument is that the measured data ΔT_{id} should be a linear function of the logarithm of time, ln t. Once the temperature rise of the hot wires is measured as a function of the time, t, the gradient of the linear function of ΔT_{id} vs the logarithm of t can be obtained; then, the thermal conductivity λ can be calculated.

Instrument

The instrument employed in this work is shown in Figure 1. The outer part is a pressure vessel made of stainless steel and designed for an operating pressure of 60 MPa and operating temperature range from 230 K to 350 K. The inner cell in which the hot-wires are mounted is composed of two compartments formed by machining two identical holes centering on the split diameter of a copper cylinder and parallel to its axis. The half of the cylinder shown in Figure 1 carries the five wire supports and is itself supported by the aluminum ring located in the outer pressure vessel.

In this instrument, two 25 μm tantalum wires were used to act as the hot wires (13.8 cm and 4.6 cm in length) and were anodized *in situ* to form a layer of insulating tantalum pentoxide on their surface. All electrical connections to the wires were made of 0.8 mm diameter enamel-insulated wire which extends outside of the pressure vessel. Constant tension and verticality of the wires are achieved by a copper block at the bottom of each wire and the mass was chosen to keep the tension of the hot wires to be 25% of their yielding tension (Menashe and Wakeham, 1981). With this instrument employing two hot wires, the errors caused by the finite length can be eliminated with the compensation of the short wire to the long wire (Kestin and Wakeham, 1978).

The calibration of the wires to determine the temperature coefficient of the resistance of the tantalum wire was carried out *in situ*. The result was represented by a polynomial function of the resistance, $R(\Omega)$, of tantalum vs the absolute temperature T, over the temperature range

* To whom correspondence should be addressed.

S0021-9568(96)00245-2 CCC: $14.00

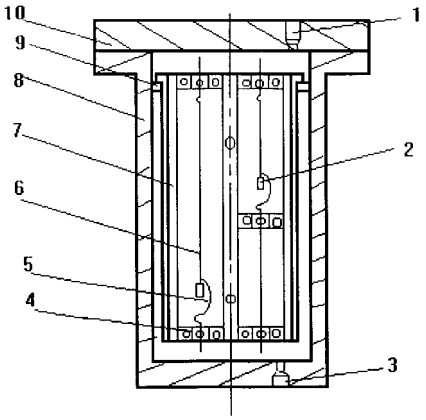

Figure 1. Instrument schematic: (1) holes for wire extension; (2) copper block; (3) tested fluid charging hole; (4) mount for wires; (5) golden strip; (6) tantalum wire; (7) copper compartment; (8) pressure vessel; (9) aluminum ring; (10) flange plate.

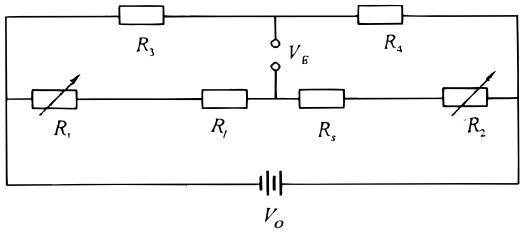

Figure 2. Unbalanced bridge employed in this work.

238.15 K to 333.15 K. The function is shown as

$$R(T) = R_0[1 + 3.5961 \times 10^{-3}(T/\mathrm{K} - 273.15) - 3.0041 \times 10^{-7}(T/\mathrm{K} - 273.15)^2] \quad (3)$$

where R_0 represents the resistance of the hot wires at the temperature of 273.15 K.

The resistance changes and thus the temperature rise of the wires were measured by an unbalanced bridge shown in Figure 2. According to this bridge, the difference of the resistance of the two wires can be written in the following form as the two wires are identical except for their length.

$$\Delta R = R_l - R_s = \left(\frac{l_l}{l_s} - 1\right)\frac{CR_1 + CR_2 - R_1}{\frac{l_l}{l_s}(1 - C) - C} \quad (4)$$

in which

$$C = \frac{V_E}{V_O} + \frac{R_3}{R_3 + R_4} \quad (5)$$

where R_l is the resistance of the long hot wire, R_s is the resistance of the short hot wire; l_l is the length of the long wire, l_s is the length of the short wire, V_O is the voltage of the power source, V_E is the voltage of the bridge measured, R_1 and R_2 are the resistance of two resistors with adjusted resistance values, and R_3 and R_4 are the resistance of two standard resistors with fixed resistance. The voltage of the bridge, V_E, was measured with the Hewlett Packard 3852A data collector and the collecting rate was about 30 points/s. The temperature rise of the hot wires was about 10 K in this work. The uncertainty of the instrument is estimated less than 3%.

Results and Analysis

On the basis of the above work, the thermal conductivities of gaseous HFC-32 and HFC-125 near the saturation line were measured. The mass purity of both samples is 99.95%. The uncertainty of the temperature measurements was within 10 mK, and the thermal gradient of the bath used in the experiment was less than 5 mK. Figure 3 shows the function of temperature rise ΔT vs the logarithm of time t for HFC-32 at the bath temperature 308.15 K. There are three parts in the curve. After careful analyses, it was found that the first part of the curve is a segment where the thermophysical properties of the hot wire shows an significant effect and the third part is a segment where the natural convection begin to appear and shows a significant effect. Figure 4 shows the linear

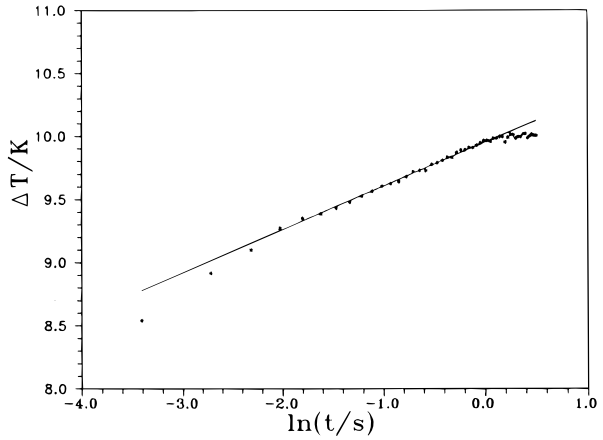

Figure 3. Temperature rise of the hot wire vs the logarithm of time.

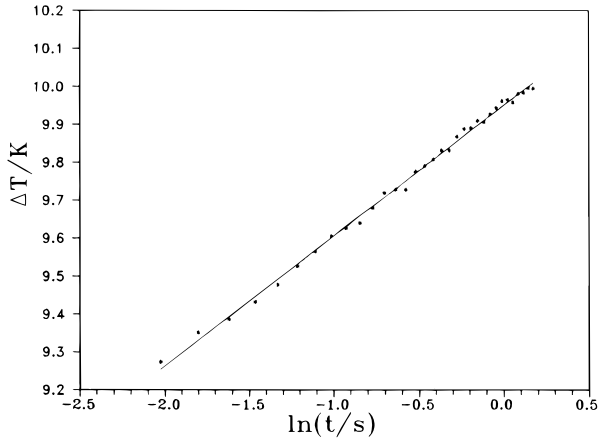

Figure 4. Linear function of the temperature rise of the hot wire vs the logarithm of time.

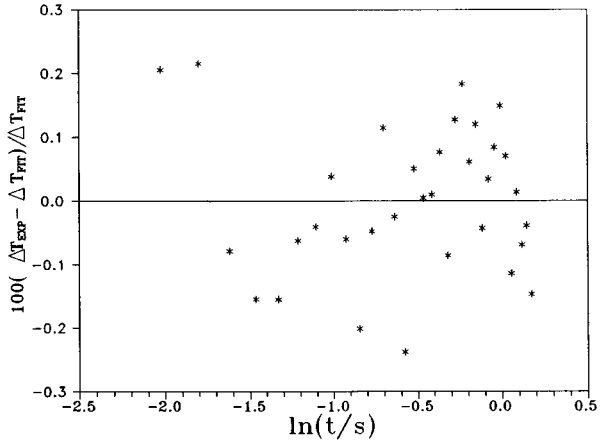

Figure 5. Deviation of the temperature rise of the hot wire from the correlated linear function.

Table 1. Coefficient of Eq 6 for HFC-32 and HFC-125

	D_0/W·m^{-1}·K^{-1}	D_1/W·m^{-1}·K^{-2}	D_2/W·m^{-1}·K^{-3}	D_4/W·m^{-1}·K^{-4}
HFC-32	1.28553×10^{-2}	6.17729×10^{-5}	-5.38075×10^{-7}	1.51692×10^{-8}
HFC-125	1.21765×10^{-2}	1.05989×10^{-4}	2.37973×10^{-7}	8.93820×10^{-9}

Table 2. Thermal Conductivity of Gaseous HFC-32

T/K	P/MPa[a]	λ/W·m^{-1}·K^{-1}	T/K	P/MPa[a]	λ/W·m^{-1}·K^{-1}
254.51	0.2214	0.011 49	300.75	1.280	0.014 63
258.77	0.2734	0.011 79	305.31	1.474	0.014 82
263.37	0.3345	0.012 18	309.68	1.690	0.015 09
267.44	0.4055	0.012 41	313.48	1.928	0.015 48
271.80	0.4878	0.012 71	319.06	2.190	0.015 76
275.54	0.5822	0.012 97	322.17	2.479	0.016 45
280.00	0.6901	0.013 35	326.75	2.796	0.017 00
287.47	0.8126	0.013 62	331.78	3.143	0.017 68
291.80	0.9509	0.014 02	337.50	3.521	0.018 51
296.41	1.106	0.014 10	341.76	3.934	0.019 67

[a] Calculated with NIST REFPROP Program (Version 4.01).

Table 3. Thermal Conductivity of Gaseous HFC-125

T/K	P/MPa[a]	λ/W·m^{-1}·K^{-1}	T/K	P/MPa[a]	λ/W·m^{-1}·K^{-1}
251.21	0.1853	0.009 41	293.07	0.9087	0.014 24
255.59	0.2285	0.010 24	297.59	1.049	0.014 83
260.11	0.2791	0.010 71	303.35	1.204	0.015 67
264.38	0.3379	0.011 38	307.85	1.776	0.017 70
269.80	0.4056	0.011 83	320.61	2.006	0.018 68
274.68	0.4831	0.012 29	325.11	2.257	0.019 78
279.07	0.5712	0.012 88	329.75	2.533	0.020 70
283.38	0.6709	0.013 43	333.70	2.836	0.021 26
288.58	0.7831	0.014 09			

[a] Calculated with NIST REFPROP Program (Version 4.01).

function of temperature rise ΔT vs the logarithm of time t for HFC-32 at this temperature. In Figure 5 the percentage deviations of the experimental temperature rise from this linearity as a function of the logarithm of time are shown for a typical run of HFC-32 at 308.15 K. No curvature or systematic trend is apparent, and the maximum deviation is less than 0.3%. Similar deviation plots were obtained for measurements described in this paper. The lack of any curvature or systematic trend as well as the magnitude of the deviation indicates that for the temperature range considered, no radiation correction is necessary (Nieto de Castro, 1991).

The bath temperature range is 238.15 K to 333.15 K for HFC-32 and 238.15 K to 328.15 K for HFC-125. The reference temperature range is 254.51 K to 341.76 K for HFC-32 and 251.21 K to 333.70 K for HFC-125.

The measured thermal conductivities of both HFC-32 and HFC-125 were fitted to the following equation

$$\lambda = D_0 + D_1(T/\mathrm{K} - 273.15) + D_2(T/\mathrm{K} - 273.15)^2 + D_3(T/\mathrm{K} - 273.15)^3 \quad (6)$$

the values of the coefficients in eq 6 for HFC-32 and HFC-125 are shown in Table 1. The standard deviation of experimentally measured data from eq 6 is 0.37% for HFC-32 and 0.43% for HFC-125. The experimentally measured data were shown in Tables 2 and 3. The pressure was calculated with the NIST program REFPROP, Version 4.01 (Gallagher et al., 1989), with the estimated accuracy of 0.5%. Figures 6 and 7 show the deviations of the experimental results of thermal conductivity of HFC-32 and HFC-125 in this work and in the literature from eq 6 separately, where λ represents the experimental results and λ_{FIT} are the values calculated from eq 6. The compared results in the literature are those whose thermodynamical state is

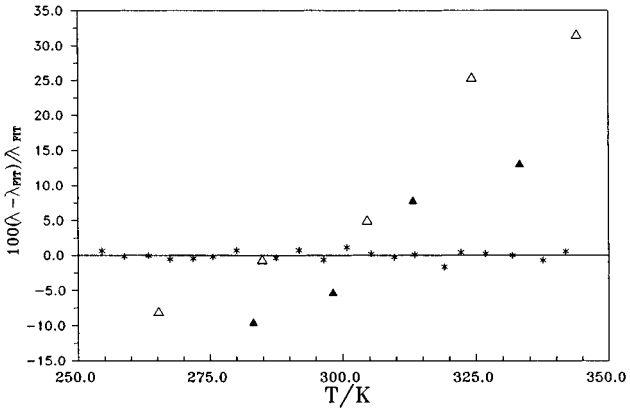

Figure 6. Comparisons of the thermal conductivity of HFC-32 of different authors with eq 6: (▲) Tanaka et al.; (△) Gross et al.; (*) this work.

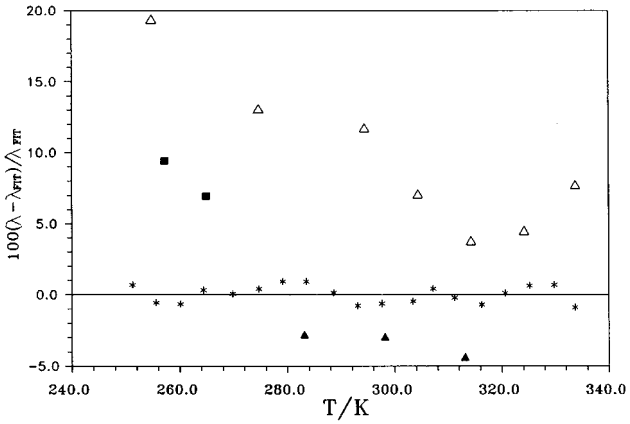

Figure 7. Comparisons of the thermal conductivity of HFC-125 of different authors with eq 6: (▲) Tanaka et al.; (■) Tsvetkov et al.; (△) Gross et al.; (*) this work.

very close to that of the results in this work. The maximum deviation of the experimental results of this work for both fluids from eq 6 is no more than 1%. The compared results of HFC-32 by Tanaka et al. (1995) include those at 0.80 MPa of the 283.15 K isotherm, 1.10 MPa of 298.15 K isotherm, 2.00 MPa of 313.15 K isotherm, and 3.00 MPa of 333.15 K isotherm. The compared results of HFC-125 by Tanaka et al. (1995) include those at 0.70 MPa of the 283.15 K isotherm, 1.10 MPa of the 298.15 K isotherm, and 1.60 MPa of the 313.15 K isotherm. The compared results of HFC-32 by Gross and Song (1996) include those at 0.331 MPa of the 265.25 K isotherm, 0.774 MPa of the 284.84 K isotherm, 1.284 MPa of the 304.55 K isotherm, 2.616 MPa of the 324.25 K isotherm, and 39.62 MPa of the 343.95 K isotherm. The compared results of the HFC-125 by Gross and Song (1996) include those at 0.220 MPa of the 254.75 K isotherm, 0.447 MPa of the 274.65 K isotherm, 1.093 MPa of the 294.35 K isotherm, 1.120 MPa of the 304.35 K isotherm, 1.568 MPa of the 314.25 K isotherm, 2.070 MPa of the 324.15 K isotherm, and 27.30 MPa of the 333.75 K isotherm. The compared results of HFC-125 by Tsvetkov et al. (1995) include those at 0.30 MPa of the 257.21 K isotherm and 0.31 MPa of the 264.90 K isotherm. The maximum deviation of the results by Tanaka et al. (1995) from eq 6 is about 15% for HFC-32 and 5% for HFC-125. The maximum deviation of the resutls by Gross and Song

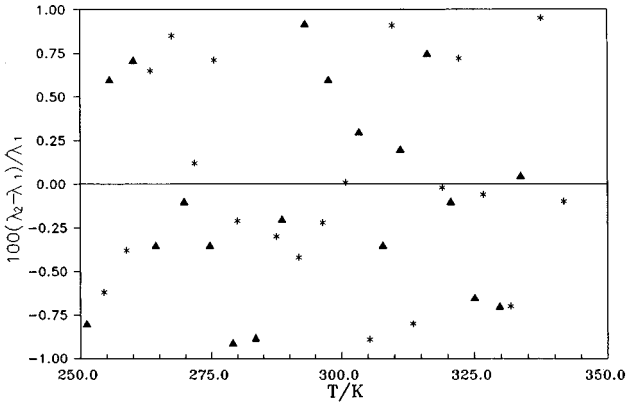

Figure 8. Comparisons of the results of repetitious experiments from primary results: (*) comparisons for HFC-32; (▲) comparisons for HFC-125.

(1996) from eq 6 is 33% for HFC-32 and 20% for HFC-125. The maximum deviation of the results by Tsvetkov et al. (1995) from eq 6 is 10% for HFC-125. Figure 8 shows the deviations of the results of repetitious experiment from the primary results, where λ_2 represents the results of repetitious experiment and λ_1 represents the primary results. The maximum deviation of repetitious experiment results from primary results is no more than 1% for both fluids.

Conclusion

An instrument with two hot wires for measurement of thermal conductivity of fluids was constructed and the thermal conductivity of gaseous HFC-32 and HFC-125 near the saturation line was measured with an uncertainty of less than 3%.

Acknowledgment

We are indebted to Zhejiang Fluoro-Chemical Technology Research Institute and ICI Co. for furnishing samples of HFC-32 and HFC-125, respectively.

Literature Cited

Gallagher, J.; McLinden, M.; Morrison, G.; Huber, M. *NIST Thermodynamic Properties of Refrigerants and Refrigerants Mixtures, Version 4.01*; NIST Standard Reference Database 23; NIST: Washington, DC, 1989.

Gross, U.; Song, Y. W. Thermal Conductivities of New Refrigerants R125 and R32 Measured by the Transient Hot-Wire Method. *Int. J. Thermophys.* **1996**, *17*, 607−619.

Healy, J. J.; De Groot, J. J.; Kestin, J. The Theory of the Transient Hot-wire Method for Measuring Thermal Conductivity. *Physica* **1976**, *82C*, 392−408.

Kestin, J.; Wakeham, W. A. A Contribution to the Theory of the Transient Hot-wire Technique for Thermal Conductivity Measurements. *Physica* **1978**, *92A*, 102−116.

Menashe, J.; Wakeham, W. A. Absolute Measurements of the Thermal Conductivity of Liquids at Pressures up to 500 MPa. *J. Phys. Chem.* **1981**, *85*, 340−347.

Nieto de Castro, C. A.; Perkins, R. A.; Roder, H. M. Radiative Heat Transfer in Transient Hot-wire Measurements of Thermal Conductivity. *Int. J. Thermophys.* **1991**, *12*, 985−997.

Tanaka, Y.; Matsuo, S.; Taya, S. Gaseous Thermal Conductivity of Difluoromethane (HFC-32), Pentafluoroethane (HFC-125), and Their Mixtures. *Int. J. Thermophys.* **1995**, *16*, 121−131.

Tsvetkov, O. B.; Kletski, A. V.; Laptev, Y. A.; Asambaev, A. J.; Zausaev, I. A. Thermal Conductivity and PVT Measurements of Pentafluoroethane (Refrigerant HFC-125). *Int. J. Thermophys.* **1995**, *16*, 1185−1192.

Received for review July 17, 1996. Accepted October 16, 1996.[⊗]

JE960245K

[⊗] Abstract published in *Advance ACS Abstracts*, December 1, 1996.